

Modelling of Light Extinction by Soot Particles

Zhang Q.^a, Rubini P.A.

Department of Engineering, University of Hull, Kingston-upon-Hull, HU6 7RX, UK

^a *Current address: Geodata S.p.A, Corso Duca degli Abruzzi 48/E, Turin, Italy*

Corresponding author: p.a.rubini@hull.ac.uk +44(0) 1482 465818

Abstract –A simplified model for the prediction of light extinction through combustion generated smoke is presented. The model builds upon existing theory and available experimental data to account for the principal factors that influence light extinction in participating media, including wavelength, primary particle size distribution, morphological structure of particle aggregation as well as multiple scattering among particles within a particle aggregation. Good agreement is demonstrated between the model predictions and experimental data in the visible and IR range. The model illustrates that as the mean particle size increases, the integral optical property of a soot cloud approaches that of monodisperse particles. It is postulated in the current study that the number of particles participating in multiple scattering is around 20 regardless the real size of particle aggregation.

Keywords: *light extinction, scattering, soot particle, fire smoke.*

Nomenclature

c_{ext}	Cross section of extinction (m^2)	n	Real part of m
\bar{c}_{ext}	Mean cross section of extinction (m^2)	n_f	Number density of free electrons
d_m	Most probable particle diameter (m)	n_j	Number density of j-th bound electrons
d_p	Primary particle diameter (m)	n_p	Number of particles in a soot aggregation
D_f	fractal dimension	N	Number density of primary particles
f_v	Soot mass concentration	$p(d_p)$	pdf for particle size distribution
g_f	Damping constant of the free electron	p_0	Normalisation constant of $p(d_p)$
g_{bj}	Damping constant of the j-th bound electron	Q_{abs}	Absorption efficiency
I	Irradiance ($watt/m^2$)	Q_{ext}	Extinction efficiency
k_f	Imaginary part of m	Q'_{ext}	Extinction efficiency modified by multiple scattering
k_{ext}	Mass specific extinction coefficient (m^2/g)	Q_{sca}	Scattering efficiency
k	Prefactor of RDG model	R_g	Radius of gyration of a particle aggregate (m)
l	length of light path (m)	x_m	Most probable size parameter
m	Refractive index	x_p	particle size parameter
M_i	The i-th moment of the pdf for particle size distribution		
M_s	Soot mass concentration in unit volume of smoke (g/m^3)		

Greek

α_{ext}	Volumetric extinction coefficient (1/m)	ρ_p	Scattering to absorption ratio of primary
κ	Wave number		particle
λ	Wavelength (m)	σ	Geometric standard deviation
ρ_p	Soot density (g/m ³)	ω	Angular frequency
ρ_s	Scattering to absorption ratio of aggregate	ω_{bj}	Natural frequency of j-th bound electron

Introduction

The scattering of light by particulates has been studied for over a century, commencing with Clebsch in 1861, even before Maxwell had proposed his electromagnetic theory. Lord Rayleigh applied Maxwell’s equations and formally established the theory of Rayleigh scattering in 1881. Other notable contributors have included Lorenz in 1890, Debye in 1909 and Mie in 1908. The latter two extended Rayleigh’s theory to incorporate both larger and non-spherical particles [1].

As laser based diagnostic techniques have been introduced into combustion engineering, the determination of the optical properties of soot particles, measurement of particle size and concentration has become increasingly important. Previous studies have applied Rayleigh’s theory to monitor the mass concentration of particulates from combustion sources such as diesel engines, for example, Roessler and Faxvog [2], Scherrer, Kittalson and Dolan [3] and Japar and Szkarlat [4]. Jennings and Pinnick [5] proposed that the mass specific extinction coefficient for soot particles is only dependent on wavelength, based on the assumption that carbonaceous smoke particles are small (relative to Rayleigh criteria), homogenous and highly absorptive in the visible and IR range.

In the last two decades many studies have been reported where the mass specific extinction coefficient of smoke from hydrocarbon fuels, typical of fires, has been measured under various combustion conditions. Mulholland has summarised such work in the SFPE hand book [6]. Table 1 presents a summary of published properties of smoke from which it can be seen that the value of the extinction coefficient, k_{ext} , varies over a wide range according to the combustion environment and illumination conditions. This demonstrates that considerable uncertainty exists when selecting the extinction coefficient, k_{ext} , as an input parameter to empirical light extinction and visibility models.

In this paper existing published theoretical and empirical models for specific sub-phenomena are reviewed and a more comprehensive model for light extinction is proposed. The resultant model is simpler than a full series expansion as in traditional Mie theory and more accurate and versatile than assigning constant empirical values. Such a model is particularly important in applications such as the study of visibility in fire smoke, where there is a considerable distribution of particle size and the entire visible spectrum needs to be considered.

Single scattering by small particles and Mie scattering theory

For a single spherical particle that is illuminated by non-polarized light and which satisfies the condition of $x_p |m - 1| \ll 1$ the optical efficiencies Q can be determined by Lorenz-Mie theory as [8]

$$Q_{sca} = \frac{8}{3} x_p^4 \left| \frac{m^2 - 1}{m^2 + 1} \right|^2 \quad (1)$$

$$Q_{ext} = 4x_p \operatorname{Im} \left\{ \frac{m^2 - 1}{m^2 + 1} \left[1 + \frac{x_p^2}{15} \left(\frac{m^2 - 1}{m^2 + 1} \right) \frac{m^4 + 27m^2 + 38}{2m^2 + 3} \right] \right\} + \frac{8}{3} x_p^4 \operatorname{Re} \left\{ \left(\frac{m^2 - 1}{m^2 + 1} \right)^2 \right\} \quad (2)$$

$$Q_{abs} = Q_{ext} - Q_{sca} \quad (3)$$

where the size parameter x_p and refractive index m of the particle are defined as

$$x_p = \frac{\pi d_p}{\lambda} \quad (4)$$

$$m = \iota + k \quad (5)$$

For smaller particles, where $x_p \ll 1$ and $x_p |m - 1| \ll 1$, (1) and (2) reduce to Rayleigh scattering

$$Q_{abs} = 12x_p^4 E(m) \quad (6)$$

$$Q_{sca} = \frac{8}{3} x_p^6 F(m) \quad (7)$$

where

$$E(m) = \operatorname{Im} \left(\frac{m^2 - 1}{m^2 + 1} \right) \quad (8)$$

$$F(m) = \left| \frac{m^2 - 1}{m^2 + 1} \right|^2 \quad (9)$$

Refractive index and Drude-Lorentz model

When applying Mie scattering theory, the value of the complex refractive index, m , is required. Table 2 provides a summary of values recently reported in the literature. For soot particles, the refractive index may be affected by factors such as particulate temperature, the hydrogen to carbon ratio of the fuel, particle size distribution, the

form of aggregation of particles and the wavelength of illuminating light. Of these, the influence of temperature has been reported to be very weak [9, 10]. Charalampopoulos and Felske [11] carried out in-situ measurement of refractive index at different heights in a premixed methane/oxygen flame. With the geometric width of the particle distribution up to 1.24, no significant influence of particle size distribution on refractive index was observed.

Dalzell and Sarofim [12] developed an argument, based on the Drude-Lorentz dispersion model, that an increase in the hydrogen to carbon ratio in soot results in a decrease of the number of free electrons and a decrease in both the real and the imaginary part of the refractive index. They reported results with acetylene and propane however did not show any significant differences to support their argument. Wu, Krishnan and Faeth [13] have since confirmed that refractive index does not vary significantly between different fuel types. The effect of the morphology of particle aggregation on the optical properties of soot is discussed in the following section.

The dependence of refractive index on wavelength is evident in both experiments and theoretical models, including for example, Dalzell and Sarofim [12], Wu, Krishnan and Faeth [13], Lee and Tien [14], Batten [15], Charalampopoulos [11], Chang and Charalampopoulos [16]. One of the most widely used models that demonstrates this is the Drude-Lorentz dispersion model [14], which may be defined as

$$n^2 - \epsilon^2 = + \frac{e^2}{m_e \epsilon} \sum_{j=1}^{\infty} \frac{n_j (\omega_{bj} - \omega)}{\omega_{bj} - \omega + \omega_{bj}^2} - \frac{e^2}{m_e^0 \epsilon} \frac{n_f}{\omega + \gamma_f^2} \quad (10)$$

$$2nk = \frac{e^2}{m_e \epsilon} \sum_{j=1}^{\infty} \frac{n_j \omega_{bj}}{\omega_{bj} - \omega + \omega_{bj}^2} - \frac{e^2}{m_e^0 \epsilon} \frac{n_f \gamma_f}{\omega + \gamma_f^2} \quad (11)$$

where, e is the electron charge, ϵ is the permittivity, m_e is the electron mass in vacuum and m_e^0 is the effective electron mass. n_j 's and n_f are the bound and free electron number densities, ω_{bj} is the natural frequency of bound electrons with $\omega_{b1} = 1.25 \times 10^{15}$ and $\omega_{b2} = 7.25 \times 10^{15}$. The values are the same for all the models. ω is the frequency, g_{bj} and g_f are the damping constants of the bound and free electrons. Except in the model by Lee and Tien, m_e is used for both the free and bound electrons. Table 4 summarises the values of the number density, n , and damping constant, g , employed in the above models. A similar model for refractive index was also proposed by Stull and Plass [9].

The variations of refractive indices with wavelength from the above models are shown in Fig.1. It can be seen that the model by Lee and Tien [14] is most sensitive and the model by Stull and Plass [9] is least sensitive to the effect of resonance. Fig.2 compares the resulting extinction efficiency from Mie scattering with the three dispersion models for refractive index. The model of Dalzell appears to most closely follow the experimental measurements of Q_{ext} by Chang and Charalampopoulos [16].

Light scattering by aggregates of soot particles

In combustion generated smoke, soot particles rarely exist in isolation, rather forming chain-like aggregates [17]. The optical properties of the resulting aggregates are significantly different from those of the individual soot particles. Berry and Percival [18] studied the theory of fractal aggregate optics and found that the scattering cross section of the aggregate is different for $D_f > 2$ from that of $D_f < 2$ where D_f is the fractal dimension. For smoke ($D_f < 2$), the scattering per primary particle can exceed that of a solitary particle by a factor of $x_p^{-3-D_f}$. After neglecting multiple scattering, Berry and Percival found the absorption per primary particle to be unchanged from Mie scattering theory. A more practical and common model, known as the RDG (Rayleigh–Debye–Gans) model for light scattering by the aggregation of soot particles has been proposed by Dobbins and Megaridis [19]. In this model the soot aggregate is modeled as a porous sphere. Applying the Lorenz-Lorentz relation, the equivalent scattering efficiency is expressed as

$$Q_{sca} = \frac{8}{3} x_p^4 F(m) Y_a \quad (12)$$

In the power-law regime ($\kappa \overline{R_g^2} \gg 1$)

$$Y_a = k_f \left(\frac{3D_f}{6x_p} \right)^{D_f/2} \quad (13)$$

where $\kappa = 2\pi/\lambda$, k_f is a prefactor and R_g is the radius of gyration of the aggregate. Since multiple scattering has been ignored, the absorption efficiency continues to be expressed by (6) when the size of the primary particle satisfies the Rayleigh condition.

A similar analysis was carried out by Köylü and Faeth[21]. Also in the power-law regime, they gave Y_a as:

$$Y_a = k_f (4x_p)^{-D_f} \left[\frac{3}{2-D_f} - \frac{12}{(6-D_f)(4-D_f)} \right] \quad (14)$$

Although Dobbins and Megaridis [19] initially proposed a value for k_f as 5.8 and for D_f between 1.7 – 1.9, other values also exist either from direct morphological structure measurements or indirect optical measurements as summarised in Table 3. These suggest some uncertainty in the model itself though may also be the result of the incompleteness of the extinction model used by ignoring other influential effects such as particle dispersion and multiple scattering.

Polydisperse particles

In the preceding section, soot particles were assumed to be monodisperse. In reality, they are likely to be polydisperse [22, 17]. In the following analysis a zeroth-order logarithmic distribution (ZOLD) [1] is adopted,

which is an alternative form of the more general log-normal distribution function [45], commonly employed in aerosol science [46]. This may be defined as,

$$p(d_p) = \frac{p_0}{d_m} \exp\left[-\frac{\ln^2(d_p/d_m)}{2\sigma^2}\right] \quad (15)$$

where d_m is the modal value of d_p and σ is the geometric width of $p(d_p)$, a dimensionless measure of width and skewness. These two parameters are readily related to the mean and true standard deviation [44]. The normalization constant, p_0 is defined as

$$p_0 = \frac{1}{\sqrt{2\pi}} \exp\left(-\frac{\ln^2 \sigma}{2}\right) \quad (16)$$

Fig.3 shows the comparison between ZOLD prediction and experimental data from Mulholland [6]. The i -th moment of $p(d_p)$ is

$$M_i = \int d_p^i p(d_p) dd_p = d_m^i \exp\left\{\left[i+1\right] - 1 \frac{\ln^2 \sigma}{2}\right\} \quad (17)$$

The average geometric cross section area of the particles is given as

$$\bar{s} = \int_0^\infty \frac{\pi}{4} d_p^2 p(d_p) dd_p = \frac{\pi}{4} d_m^2 \exp(4 \ln^2 \sigma) \quad (18)$$

Defining M_{i-2} as

$$M_{i-2} = \exp\left\{\left[i+1\right]^2 - 9 \frac{\ln^2 \sigma}{2}\right\} \quad (19)$$

The optical efficiencies for polydisperse particle can be given as

$$Q_{ext} = \frac{\bar{c}_{exts}}{\bar{s}} = 4x_p \operatorname{Im}\left\{\frac{m^2 - 1}{m^2 + 1}\left[M_3 + \frac{x_p^2}{15}\left(\frac{m^2 - 1}{m^2 + 1}\right)\frac{m^4 + 7m^2 + 8}{2m^2 + 1}M_5\right]\right\} + \frac{8}{3}x_p^4 \operatorname{Re}\left\{\left(\frac{m^2 - 1}{m^2 + 1}\right)\right\}M_6 \quad (20)$$

$$Q_{sca} = \frac{\bar{c}_{sca}}{\bar{s}} = \frac{8}{3}x_m^4 F(m) Y_a M_6 \quad (21)$$

where Y_a is defined by (13) or (14) according to the scattering regime and x_m is defined by d_m . Again, Q_{abs} is defined by (3). Rayleigh scattering ($Y_a = 1.0$) and monodisperse particles ($M_{i,2}=1.0$) can be treated as special cases.

Assessment of extinction coefficient models

Fig.4 collectively presents the experimental data from the sources identified in Table 1, that can be reliably expressed in the form of $Q_{ext}=f(x_p)$. In the same figure, the curves represent predictions from the existing extinction models with constant refractive indices. The two limiting refractive indices $m=1.3+0.3i$ and $m=2.0+1.5i$ were chosen from Table 2 while $m=1.57+0.56i$ is the most popularly quoted value in the literature [13, 19, 21, 28, 29, 30, 31]. All experimental data fall into a region between the curves representing Mie scattering with $m=1.3+0.3i$ and that representing power-law regime with $m=1.57+0.56i$.

There are two features of the experimental data that can be recognised in Fig.4. The first are the peaks shown by the data from Chang and Charalampopoulos [16] due to resonance of the refractive index in the ultraviolet region (see Fig.2). The second feature is the clear separation of data into two groups. In the first group, x_p is between 0 and 0.4. In the second group x_p is larger than 0.2. The two groups of data overlap between $x_p=0.2$ and $x_p=0.4$ where Q_{ext} has multiple values for x_p .

It is generally believed that the two groups of data are the result of two morphological regimes: Guinier and power-law according to their resultant scattering angle. In Fig.4 there is one prediction curve for each regime in the RDG model with constant refractive index. What is not clear is the condition leading to each regime. The obvious cause is the change of size parameter x_p as demonstrated by the data from Chang and Charalampopoulos [16]. As x_p crosses the value about 0.3, Q_{ext} changes from one regime to another. In the transition area, Q_{ext} is a multiple value function, which indicates other causes behind it. Different fuels and the types of combustion were considered as they may produce different structure of carbonaceous aggregates. Examining the data in Fig.4, we can see that the scattering result by soot particles generated from the same kind of fuel can be seen in both regimes. The typical example is again the data from Chang and Charalampopoulos in which case soot was produced by rich premixed propane flame. Another example is shown in Fig.5 for a lean Ethylene turbulent diffusion flame. In this case, the three sets of data were generated by different people, at different times from the same research group and under otherwise almost identical conditions. The results cross both regimes. Furthermore, all three sets of result shown have the same primary particle size of $0.32\mu\text{m}$ [13, 21, 32].

Fig.4 has demonstrated that existing models are able to capture the general trend of light scattering except in the ultraviolet region. The practical problem remains how to select an appropriate refractive index, which for Mie scattering results in considerable uncertainty in the predicted values. For the RDG model, it can be seen in Fig.4 that the commonly used refractive index ($1.57+0.56i$) leads to over prediction in the Guinier regime. Multiple models for refractive index are necessary for prediction over wider practical ranges of x_p but the cut-off area is so wide that the predicted result can be very uncertain.

A unified composite model for extinction coefficient

As demonstrated in Fig.4, current models are limited in their ability to interpret the peaks and multiple values of the extinction curve. Even within the infrared and visible wavelength range, errors of 20% to 50% may occur. A unified model for the prediction of light extinction in combustion generated smoke is proposed. The model incorporates the existing RDG model of scattering in the Guinier regime as given in (12). The effects of soot morphology and polydisperse size distributions are included through the correction to Mie scattering as in (21).

In the proposed model, the use of constant refractive indices has been replaced with Dalzell's version of the Drude-Lorentz dispersion model as given by equations (10) and (11). This is necessary in practice when the wavelength is in the visible range, or shorter, as shown in Fig. 1. The model constants are given in Table 4. Among the 6 constants in Table 4, g_2 controls the shape of the Q_{ext} curve. This is demonstrated in Fig.6 where the predictions with all 4 different values of g_2 in Table 4 are compared (scaled by a constant scaling factor of 10^{15}).

Multiple scattering by soot particles

The models considered so far have assumed that only a single scattering event will occur, implying that the particles are considered either in isolation or are widely dispersed or stick together to form a larger aggregate. Experiments [23, 24, 17] have shown that soot particle aggregation results in clusters of non-coalescent particles close but still geometrically independent to each other. Mackowski [25, 26, 27], by performing multipole analysis of the scattered electric field from such particle clusters, determined that the conventional dipole approximation used in the RDG theory may result in error of more than 20% in the predicted absorption cross section for small x_p . Under constant refractive index, Mackowski found the ratio between the single particle absorption cross section and aggregate value to increase significantly as the number of particles in an aggregate increases from 1 to 20. As the number of particles in an aggregate increases the ratio gradually becomes constant [27]. Based on this analysis, a multiplicative scaling factor for the particle absorption efficiency is proposed to account for multiple scattering. Empirical evidence [27] suggests a logarithmic function of the number of particles in a soot aggregate n_p , resulting in a modified extinction coefficient, which may be expressed as

$$Q'_{ext} = Q_{sca} + \alpha g(n_p) Q_{abs} \quad (22)$$

Comparison of unified model with experimental data

Charalampopoulos and Chang [28] measured in situ optical properties of soot particles in the visible to ultraviolet wavelength range. The result has shown that as the average particle size increases the geometric width of the particle size distribution, σ_θ , decreases (see Table 5) and the extinction behaviour of the soot approaches that of the monodispersion particles observed in the earlier work of Charalampopoulos and Felske [11]. The same effect of σ_θ on Q_{ext} can be predicted with the current model as shown in Fig.7, where the significant change of the Q_{ext} curve between $x_p=0.2$ and $x_p=0.4$ as the value of σ_θ changes from 1.0 to 1.2 occurs

as seen in the measurements by Chang and Charalampopoulos [16]. It can, at least partly, explain the multiple values of Q_{ext} function within this region in Fig.4.

The simplified model for multiple scattering in (22) indicates that the number of effectively participating particles in soot aggregates can leverage the extinction curve. According to Mackowski [27], such leveraging effect is limited to about 20 particles in an aggregate. Although larger soot aggregates have been seen in experiment (27 particles per aggregate according to Charalampopoulos and Chang [28]), not all particles in a soot aggregate may participate in the multiple scattering process, particularly in a chain structure. Fig.8 shows the effect of n_p on Q_{ext} , demonstrating that the value is indeed about 20.

Finally, the results from the proposed model are presented in Fig.9 in comparison with the experimental data of Chang and Charalampopoulos [16]. This particular data set was selected as being representative of a wide spectral range (0.2 – 6.4 μ m) and common particle sizes (0.0382 – 0.0682 μ m) as well as the availability of the required parameters such as σ_θ that is required by the model. Up to a particle size parameter, $x_p=0.6$, the model shows good agreement with the experimental data. A greater discrepancy is apparent in the case of larger average particle sizes. Even in these cases, the agreement between the prediction and measurement is still very good for particle size parameters of $x_p < 0.6$. This indicates that the deficiency of the model is largely restricted to the prediction of scattering in the ultraviolet range.

Conclusion

In summarising previous experimental data, it is evident that considerable uncertainty exists in current models of extinction even within the visible and IR wavelength range. A new unified model for light extinction has been proposed in this paper that addresses factors such as the dependency of refractive index on wavelength, particle size distribution, multiple scattering and the morphological structure of soot aggregates. Both experimental data and the current model prediction have demonstrated that these factors are influential in determine the accuracy of extinction model. Within the particle size parameter range from 0.2 to 0.4, where the existing RDG model for Guinier regime overlaps with that for the power-law regime, the current model has accurately predicted the measured extinction. In its present form, the multiple scattering model is simplistic but has successfully corrected the otherwise under prediction of light extinction due to multiple scattering.

Not only does the model show good agreement with experimental data in the visible and IR range, but it may also be used to illustrate some important trends of the extinction curve. Firstly, although on first sight the experimental data may be correlated by monotonic functions, the unified model illustrates that the extinction curve is predicted to peak in the ultraviolet region. Secondly, as the mean particle size increases, the integral optical property of a soot cloud approaches that of monodisperse particles, that is, the effects of particle size distribution become less important. Both features have been observed in the experimental data.

Acknowledgement

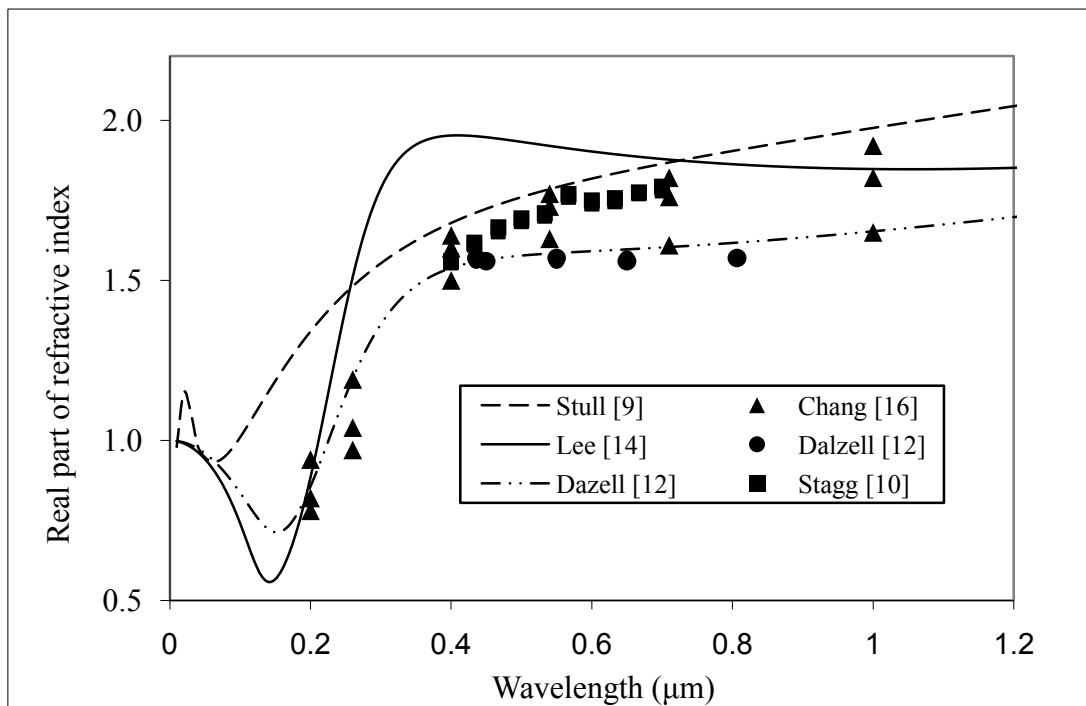
The authors gratefully acknowledge the financial support of the Engineering and Physical Sciences Research Council in the UK for this project.

References

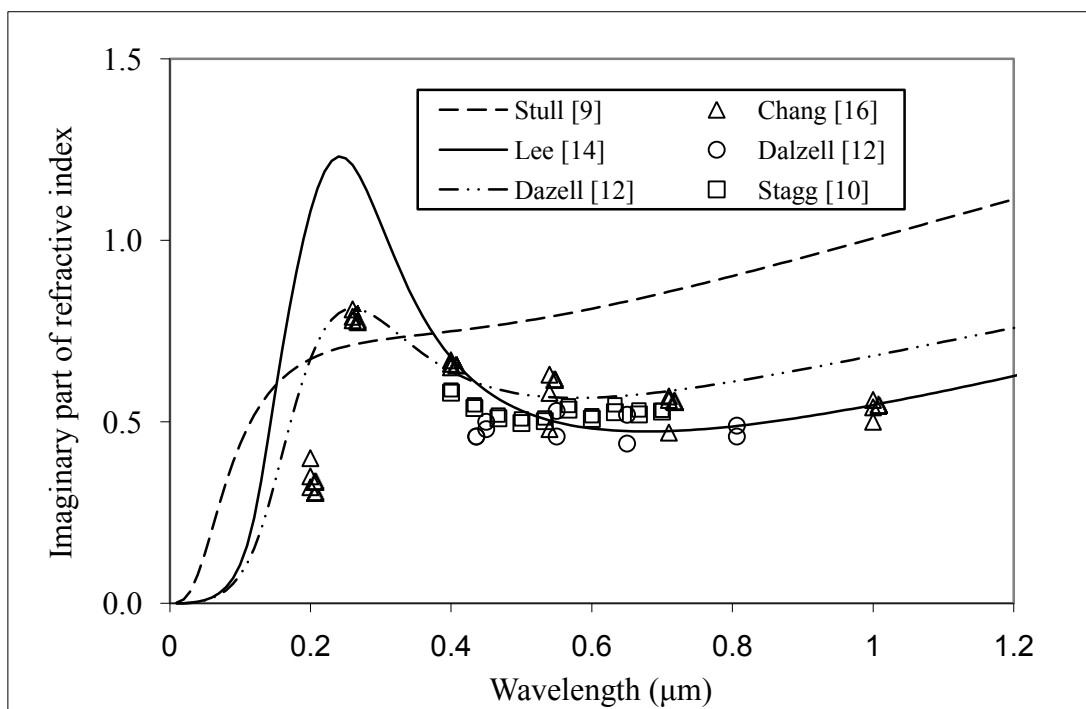
- [1] **Kerker, Milton.** *The scattering of light and other electromagnetic radiation.* New York and London : Academic Press, 1969.
- [2] **Roessler, D.M. and Faxvog, F.R.** Opacity of Black Smoke: Calculated Variation with Particle Size and Refractive Index. *Applied Optics.* 1979, Vol. 18, 9, pp. 1399-1403.
- [3] **Scherrer, H.C., Kittelson and Dolan, D.F.** Light Absorption Measurements of Diesel Particulate Matter. *SAE Paper 810181.* 1982. Society of Automotive Engineers
- [4] **Japar, S.M. and Szkarlat, A.C.** Measurement of Diesel Vehicle Exhaust Particulate Using Photoacoustic Spectroscopy. *Combustion Science and Technology.* 1981, Vol. 24, pp. 215-219.
- [5] **Jennings, S.G. and Pinnick, R.G.** Relationships between Visible Extinction, Absorption and Concentration of Carbonaceous Smoke. *Atmospheric Environment.* 1980, Vol. 14, pp. 1123-1129.
- [6] **Mulholland, G.W.** Smoke Production and Properties. *The SFPE Handbook of Fire Protection Engineering.* 2. NFPA, 2002, 2, pp. 2-258 - 2-268.
- [7] **Jones, A. R.** Light scattering for particle characterization. *Progress in energy and Combustion Science.* 1999, Vol. 25, pp. 1-53.
- [8] **Bohren, Craig F. and Huffman, Donald R.** *Absorption and Scattering of Light by Small Particles.* New York, Chichester, Weinheim, Boston, Singapore, Toronto : John Wiley & Sons Inc., 1998.
- [9] **Stull, V.R. and Plass, G.N.** Emmissivity of dispersed carbon particles. *Journal of the Optical Society of America.* 1960, Vol. 50, pp. 121-129.
- [10] **Stagg, B.J. and Charalampopoulos, T.T.** Refractive Indices of Pyrolytic Graphite, Amorphous Carbon, and Flame Soot in the Temperature Range 25° to 600°C. *Combustion and Flame.* 1993, Vol. 94, pp. 381-396.
- [11] **Charalampopoulos, T.T. and Felske, J.D.** Refractive Indices of Soot Particles Deduced from In-Situ Laser Light Scattering Measurements. *Combustion and Flame.* 1987, Vol. 68, pp. 283-294.
- [12] **Dalzell, W.H. and Sarofim, A.F.** Optical Constants of Soot and Their Application to Heat-Flux Calculations. *Journal of Heat Transfer, Trans. of ASME.* February , 1969, pp. 100-104.
- [13] **Wu, J.S., Krishnan, S.S. and Faeth, G.M.** Refractive Indices at Visible Wavelengths of Soot Emitted from Buoyant Turbulence Diffusion Flames. *Journal of Heat Transfer, Transactions of ASME.* 5 1997, Vol. 119, pp. 230-237.
- [14] **Lee, S.C. & Tien C.L.** *Optical Constants of Soot in Hydrocarbon Flames.* Eighteenth Symposium (International) on Combustion. The Combustion Institute, 1981. pp. 1159-1166.
- [15] **Batten, C.E.** Spectral optical constants of soots from polarized angular reflectance measurements. *Applied Optics.* 1985, Vol. 24, 8.
- [16] **Chang, H. and Charalampopoulos, T.T.** *Determination of the Wavelength Dependence of Refractive Indices of Flame Soot.* Proceedings: Mathematical and Physical Sciences. 1990, Vol. 430, pp. 577-591.

- [17] **Williams, J.M. and Gritz, L.A.** *In situ sampling and transmission electron microscope analysis of soot in the flame zone of large pool fires.* Twenty-Seventh Symposium (International) on Combustion. The Combustion Institute, 1998, Vol. 2, p. 2707.
- [18] **Berry, M.V. and Percival, I.C.** Optics of Fractal Clusters Such as Smoke. *Journal of Modern Optics.* 1986, Vol. 33, 5, pp. 577-591.
- [19] **Dobbins, R.A. and Megaridis, C.M.** Absorption and scattering of light by polydisperse aggregates. *Applied Optics.* 1991, Vol. 30, pp. 4747-4754.
- [20] **Mountain, R.D. and Mulholland, G.W.** Light Scattering from Simulated Smoke Agglomerates. *Langmuir.* 1988, Vol. 4, pp. 1321-1326.
- [21] **Köylü, U. O. and Faeth, G. M.** Optical Properties of Overfire Soot in Buoyant Turbulent Diffusion Flames at Long Residence Time. *Journal of Heat Transfer, Transactions of ASME.* 1994, Vol. 116, pp. 152-159.
- [22] **Köylü, U. O. and Faeth, G. M.** Structure of Overfire Soot in Buoyant Turbulent Diffusion Flames at Long residence Times. *Combustion and Flame.* 1992, Vol. 89, pp. 140-156.
- [23] **Köylü, U. O., et al.** Fractal and projected structure properties of soot aggregates. *Combustion and Flame.* 1995, Vol. 100, pp. 621-633.
- [24] **Köylü, U. O., Xing, Y. and Rosner, D.E.** Fractal Morphology Analysis of Combustion-Generated Aggregates Using Angular Light Scattering and Electron Microscope Images. *Langmuir.* 1995, Vol. 11, pp. 4848-4854.
- [25] **Mackowski, W.D.** Analysis of radiative scattering for multiple sphere configurations. *Proceedings Royal Society London.* 1991, Vol. A433, pp. 599-614.
- [26] **Mackowski.** Calculation of total cross sections of multiple-sphere clusters. *Journal of the Optical Society of America.* 1994, pp. 2851-2861.
- [27] **Mackowski.** Electrostatics Analysis of Radiative Absorption by Sphere Clusters in the Rayleigh Limit: Application to Soot Particles. *Applied Optics.* 1995, Vol. 34, 18, pp. 3535-3545.
- [28] **Charalampopoulos, T.T. and Chang, H.** In Situ Optical Properties of Soot Particles in the Wavelength Range from 340nm to 600nm. *Combustion Science and Technology.* 1988, Vol. 59, pp. 401-421.
- [29] **Dobbins, R.A., Mulholland, G.W. and Bryner, N.P.** Comparison of a Fractal Smoke Optics Model with Light Extinction Measurements. *Atmospheric Environment.* 1994, Vol. 28, 5, pp. 889-897.
- [30] **Dobbins, R.A., Santoro, R.J. and Semerjian, H.G.** *Analysis of Light Scattering from Soot Using Optical Cross Sections for Aggregates.* Twenty-Third Symposium (International) on Combustion. The Combustion Institute, 1990, pp. 1525-1532.
- [31] **Smyth, K. C. and Shaddix, C. R.** The Elusive History of $m=1.57-0.56i$ for the Refractive Index of Soot. *Combustion and Flame.* 1996, Vol. 107, pp. 314-320.
- [32] **Colbeck, I., Hardman, E.J. and Harrison, R.M.** Optical and Dynamical Properties of Fractal Clusters of Carbonaceous Smoke. *Journal of Aerosol Society.* 1989, Vol. 20, 7, pp. 765-774.
- [33] **van Hulle, P., Talbaut, M., Weill, M. and Coppalle, A.** Inversion method and experiment to determine the soot refractive index: application of turbulent diffusion flames. *Measurements Science and Technology.* 2002, Vol. 13, pp. 375-382.

- [34] **Krishnan, S.S., Lin, K.C. and Faeth, G.M.** Optical Properties in the Visible of Overfire Soot in Large Buoyant Turbulent Diffusion Flames. *Journal of Heat Transfer, Transactions of ASME*. 2000, Vol. 122, pp. 517-524.
- [35] **Suo-Anttila, Jill, et al.** An evaluation of actual and simulated smoke properties. *Fire and Materials*. 2005, Vol. 29, pp. 91-107.
- [36] **Mulholland, G.W., Henzel, V. and Babarauskas, V.** *The Effect of Scale on Smoke Emission*. Fire Safety Science - Proceedings of Second International Symposium. 1989. The National Bureau of Standards. pp. 347-357.
- [37] **Mulholland, G.W. and Choi, M.Y.** *Measurement of the Mass Specific Extinction Coefficient for Acetylene and Ethene Smoke Using the Large Agglomerate Optics Facility*. Twenty-Seventh Symposium (International) on Combustion. The Combustion Institute, 1998. pp. 1515-1522.
- [38] **Newman, J.S. and Steciak, J.** Characterization of Particulates from Diffusion Flames. *Combustion and Flame*. 1987, Vol. 67, pp. 55-64.
- [39] **Menna, P. and D'Allesio, A.** *Light Scattering and Extinction Coefficients for Soot Forming Flames in the Wavelength Range from 200nm to 600nm*. Proceedings of the 19th International Symposium on Combustion The Combustion Institute, 1982. pp. 1421-1428.
- [40] **Choi, M.Y., Mulholland, G.W., Hamins, A. and Kashiwagi, T.** *Comparisons of the Soot Volume Fraction Using Gravimetric and Light Extinction Techniques*. *Combustion and Flame*. 1995, Vol. 102, pp. 161-169.
- [41] **Patterson, R.M., Duckworth, R.M., Wyman, C.M., Powell, E.A. and Gooch, J.W.** Measurements of the Optical Properties of the Smoke Emissions from Plastics, Hydrocarbons and other Urban Fuels for Nuclear Winter Studies. *Atmospheric Environment*. 1991, Vol. 25A, 11, pp. 2539-2552.
- [42] **Colbeck, I., Atkinson, B. and Johart, Y.** *The Morphology and Optical Properties of Soot Produced by Different Fuels*. *Journal of Aerosol Society*, 1997, Vol. 28, pp. 715-723.
- [43] **Zhou, Z.Q., Ahmed, T.U. and Choi, M.Y.** Measurement of Dimensionless Soot Extinction Constant Using a Gravimetric Smapping Technique. *Experimental Thermal and Fluid Science*. 1998, Vol. 18, pp. 27-32.
- [44] **Espenscheid, W F, Kerker, M and Matijevic, E.** Logarithmic distribution functions for colloidal particles. *J. Phys. Chem.* 1964, Vol. 68., pp. 3093–3097.
- [45] **Heintzenberg, J.** *Properties of the Log-Normal Particle Size Distribution*, *Aerosol Science and Technology* 1994, Vol. 21, 1, pp.46-48.
- [46] **Hinds, W. C.** *Aerosol Technology*. Wiley Interscience, New York, 1999.



(a) Real components



(b) imaginary components

Fig. 1 – Refractive index. Comparison between the models of Stull & Plass [9], Dalzell & Sarofim [12], Lee & Tien [14] and experimental data from Chang & Charalampopoulos [16], Dalzell & Sarofim [12], Stagg & Charalampopoulos [10]

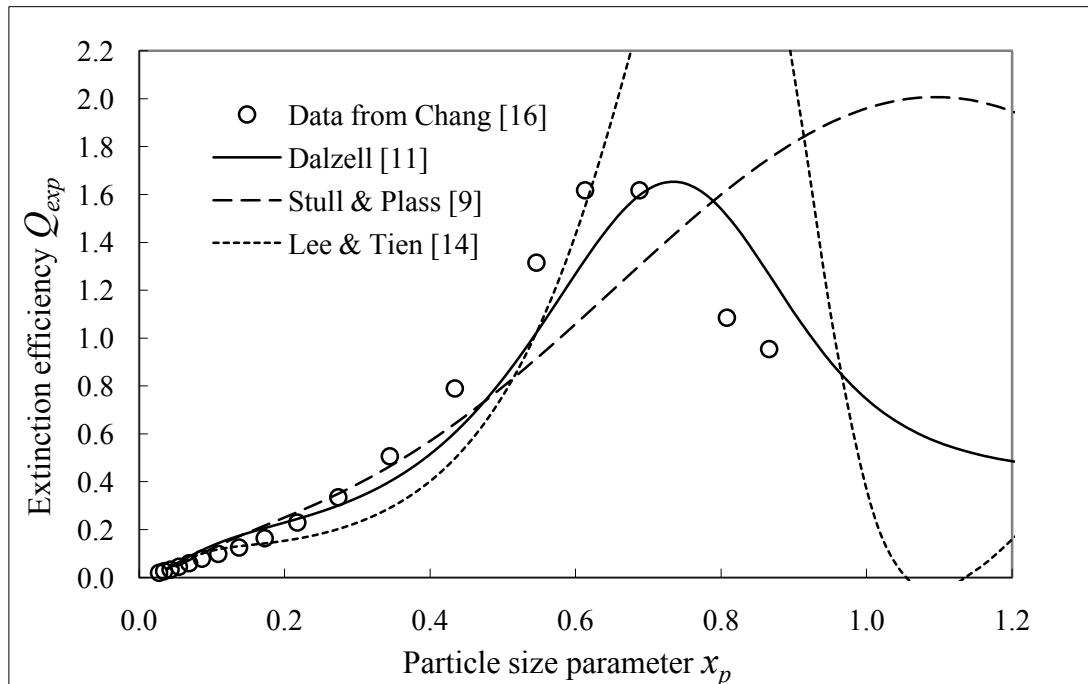


Fig. 2 - Comparison of Extinction efficiency, Q_{ext} , determined by the models of Stull & Plass [9], Dalzell & Sarofim [12], Lee & Tien [14] with the experiments of Chang and Charalampopoulos [16]

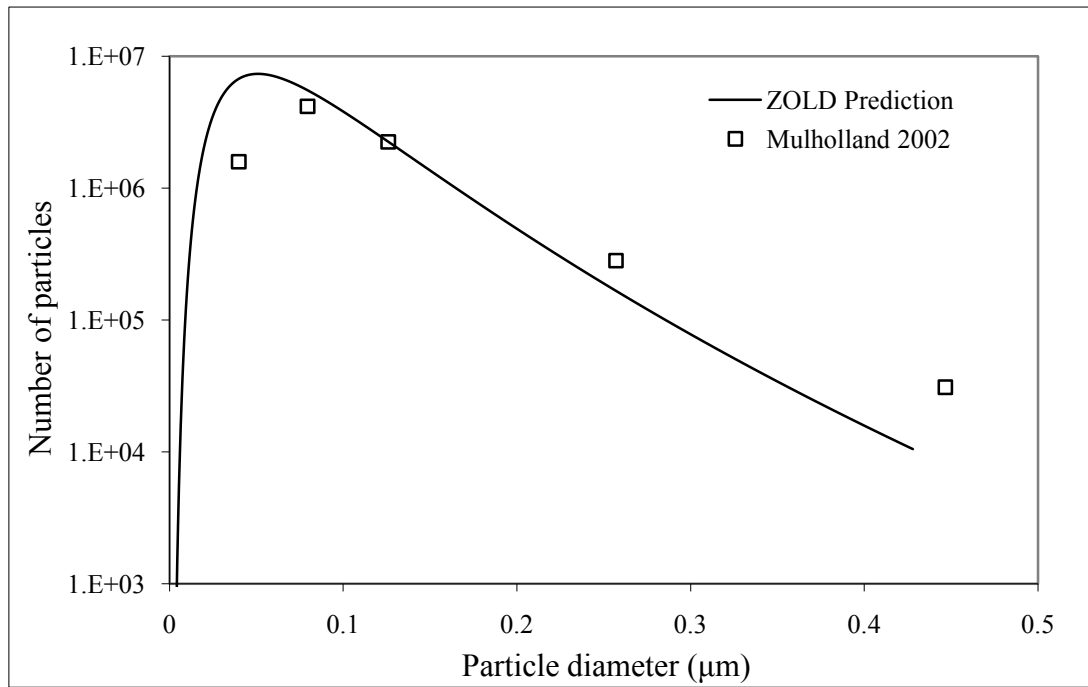


Fig. 3 – Comparison of particle size distribution from ZOLD model and experimental data of Mulholland [6]

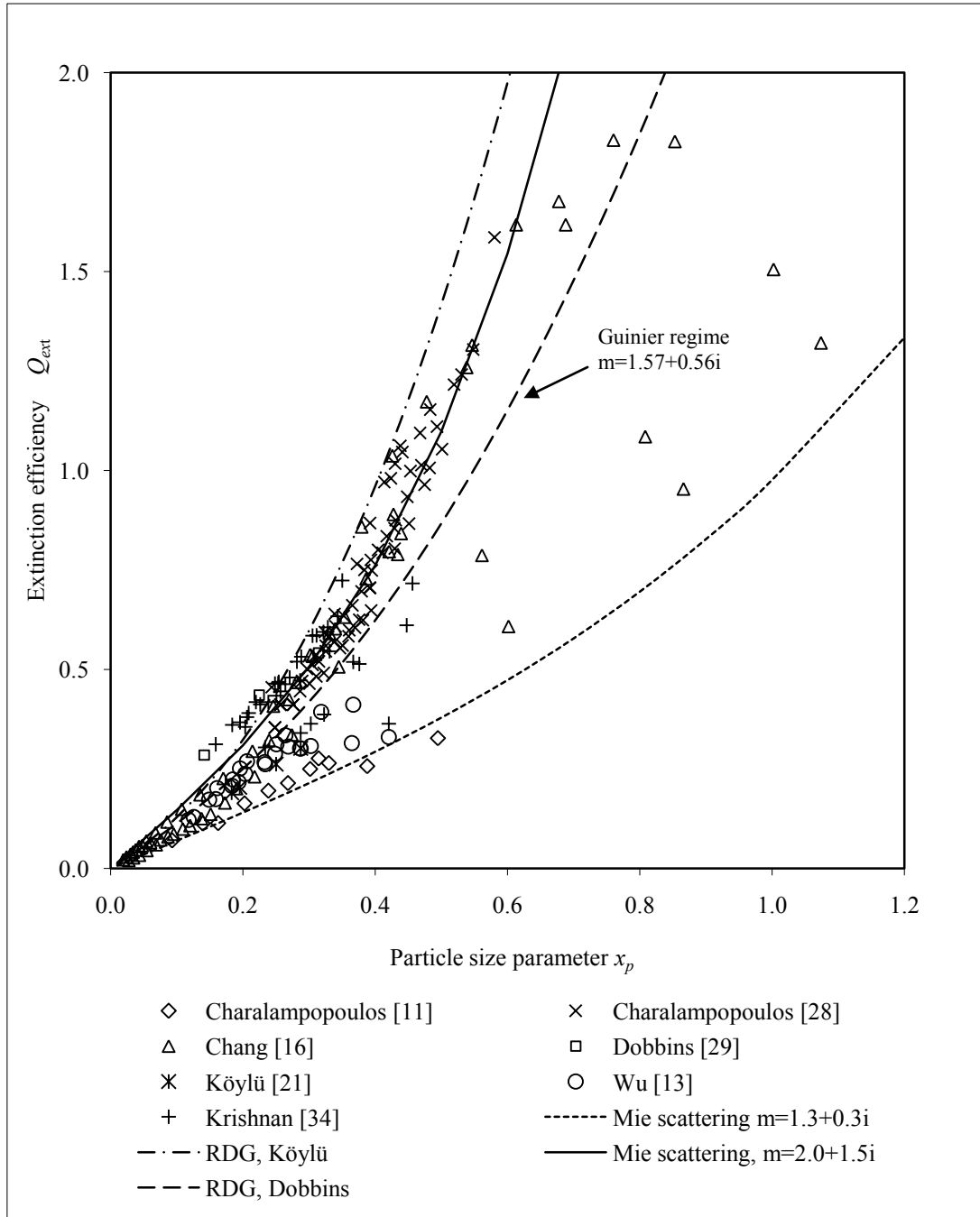


Fig. 4 - Extinction efficiency as a function of size parameter

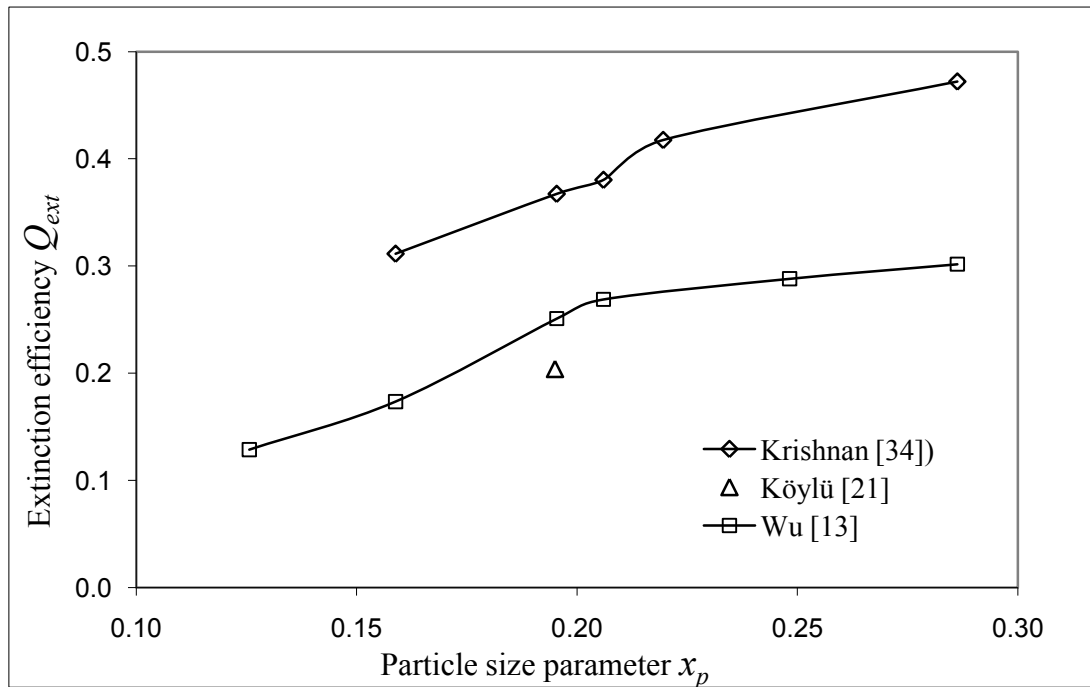


Fig. 5 - Extinction efficiency of Ethylene. Data from Krishnan [34], Köylü [21] and Wu [13]

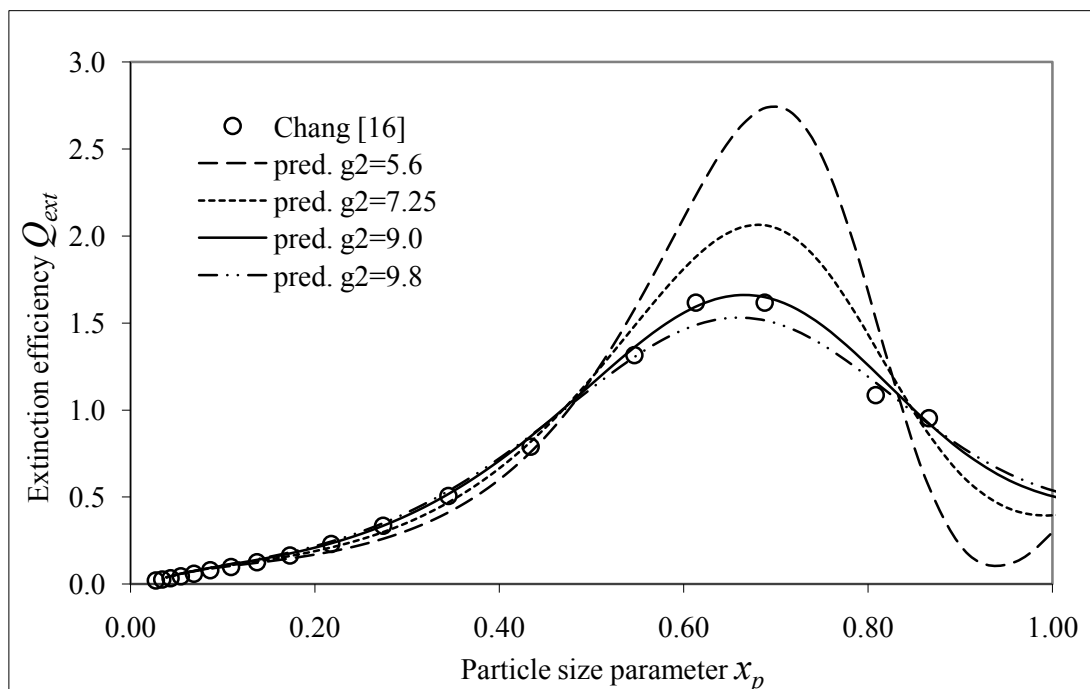


Fig. 6 - Effect of damping constant g_2 on extinction efficiency vs. experimental data of Chang and Charalampopoulos [16]

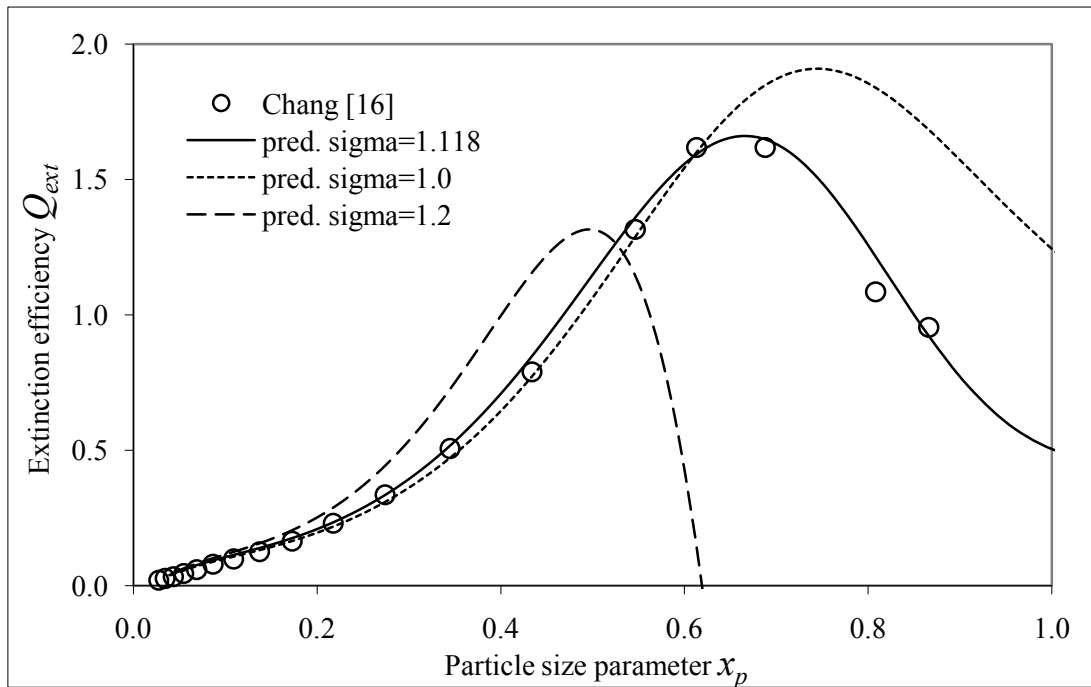


Fig. 7 - Effect of σ_p on extinction efficiency vs. experimental data of Chang and Charalampopoulos [16]

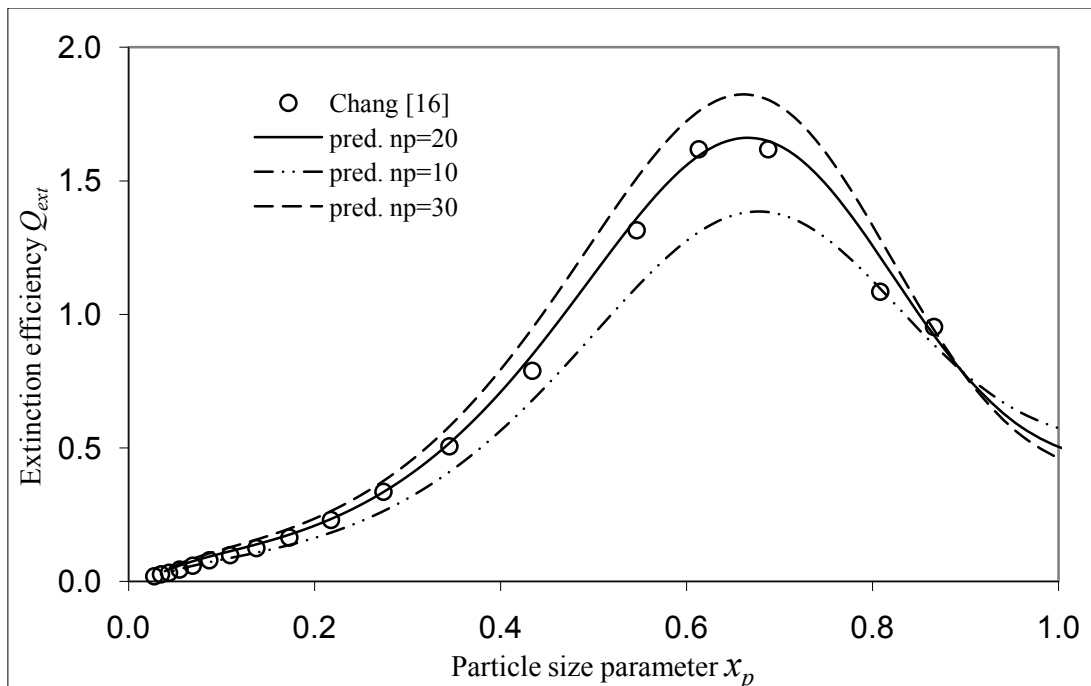


Fig. 8 - Effect of n_p on extinction efficiency vs. experimental data of Chang and Charalampopoulos [16]

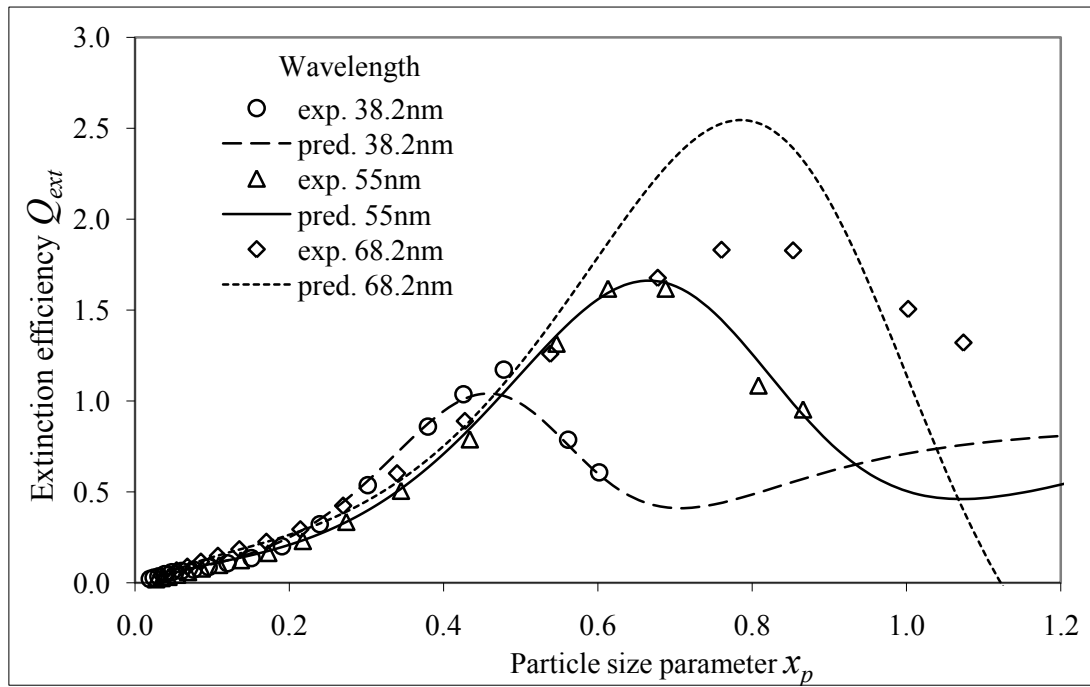


Fig. 9 - Comparison of predicted extinction efficiency from the unified model with the experimental data of Chang and Charalampopoulos [16] as a function of wavelength

No	Reported properties							Light source	Combustion	Fuel	Sampling condition	Source
	k_{ext}	d_p	N	n_p	f_v	ρ_p (g/cm ²)	m					
1	7.0 – 13							Laser	pool fire	Vary	Exhaust	[36]
2	5.1 – 9.7	y						white light	pool fire	crude oil	exhaust	[29]
3	7.8	y						laser	lam/turb diff	vary	over flame	[37]
4	4.64 – 14.3				1.1			white light	well vent. diff.	vary	exhaust	[38]
5	2 – 55 ^c							white light	rich premix	methane		[39]
6	7.6 – 8.7							laser	rich premix	acetylene	over flame	[40]
7	1.4 – 17.2							laser	pool fire	vary	in/ex situ	[41]
8	3.3 – 7.08	y	y	y	y	1.85 - 1.93	y ^b	vary	lean turb. diff.	vary	over flame	[13]
9	7.8 – 11.6							laser	rich diff. flame	vary	ex situ	[42]
10	5.1 – 5.18	y	y	y				laser	lean turb. diff.	vary	over flame	[21]
11	8.5				y	1.74		laser	rich premixed	acetylene	over flame	[43]
12	0.29 – 24.7	y	y				y	vary	rich premixed	propane	over flame	[16]
13	3.4 – 4.6	y	y				y	laser	rich premixed	methane	in situ	[11]
14	7.9 – 13.2	y						laser	rich premixed	propane	in situ	[28]
15	4.94 – 14 ^c	y	y	y	y ^a		y ^b	vary	lean turb.diff.	vary	exhaust	[34]

Table 1 – Experimentally determined mass specific extinction coefficients (6)

a - measured but value not reported; b - calculated from RDG model; c - soot density is assumed to be 1.86

No	Real part	Imaginary part	Source
1	1.56 – 4.8	0.44 – 3.82	Dalzell [12]
2	1.9 – 2.1	0.4 – 0.8	Lee & Tien [14]
3	1.2 – 1.45	0.1 – 0.27	Batten [15]
4	1.37 – 1.6	0.41 – 0.52	Charalampopoulos [11]
5	1.52 – 1.82	0.65 – 0.88	Charalampopoulos [28]
6	0.78 – 4.09	0.32 – 3.37	Chang & Charalampopoulos [16]
7	1.2 – 2.0	0.1 – 1.0	Horvath [44]
8	1.55 – 2.10	0.55 – 1.0	Dobbins [19, 29, 30]
9	1.57	0.56	Wu [13]
10	1.95 – 2.5	0.45 – 0.51	Van Hulle [33]
9	1.55 – 1.9	0.55 – 0.8	Suo-Anttila [35]

Table 2 - Published values of refractive index of soot particles

No	D_f	k_f	Source
1	1.89 – 2.07		Mountain & Mulholland [20]
2	1.6 – 1.8	9	Dobbins [29]
3	1.7 – 1.9	5.8	Dobbins & Megaridis [19]
4	1.77	8.5	Wu, Krishnan and Faeth [13]
5	1.12 – 2.35		Colbeck, Hardman and Harrison [32]
6	1.4 – 2		Jones [7]
7	1.75	20	van Hulle et al [33]
8	1.77 – 1.80	8.5	Krishnan, Lin and Faeth [34]
9	1.56 – 1.71	7.15 – 7.59	Suo-Anttila et al [35]

Table 3 - Published values of fractal dimension, D_f , and k_f , the imaginary component of the refractive index, m

	Number density (n)			Damping constant (g)		
	n_f	n_1	n_2	g_f	g_1	g_2
Dalzell and Sarofim [12]	4.06×10^{27}	2.69×10^{27}	2.86×10^{28}	6.0×10^{15}	6.0×10^{15}	7.25×10^{15}
Lee and Tien [14]	4.0×10^{25}	4.07×10^{27}	4.47×10^{28}	1.2×10^{15}	5.9×10^{15}	5.6×10^{15}
Charalampopoulos [28]	4.82×10^{25}	3.88×10^{27}	$11 n_1 - n_f$	1.2×10^{15}	6.1×10^{15}	9.8×10^{15}
Present study	4.82×10^{25}	2.69×10^{27}	$11 n_1 - n_f$	6.0×10^{15}	6.1×10^{15}	9.0×10^{15}

Table 4 - Number densities and damping constants in Drude-Lorentz model

Particle diameter	38nm	55nm	68nm
Charalampopoulos and Chang [28]	1.197	1.155	1.142
Present study	1.164	1.118	1.1

Table 5 - Variation of particle size distribution, σ